Title

Targeting PLOD2 suppresses invasion and metastatic potential in radiorecurrent prostate cancer

Journal

BJC Reports, 2(1)

ISSN

2731-9377

Authors

Frame, Gavin
Leong, Hon
Haas, Roni
et al.

Publication Date

2024

DOI

10.1038/s44276-024-00085-3

Peer reviewed

BJC reports www.nature.com/bjcreports

ARTICLE OPEN

Check for updates

Targeting PLOD2 suppresses invasion and metastatic potential in radiorecurrent prostate cancer

Gavin Frame[1,2], Hon Leong[1,2], Roni Haas[3], Xiaoyong Huang[2], Jessica Wright[1,2], Urban Emmenegger[2,4], Michelle Downes[2,5], Paul C. Boutros[3], Thomas Kislinger[1,6] and Stanley K. Liu[1,2,7]✉

BACKGROUND: Metastatic relapse of prostate cancer after radiotherapy is a significant cause of prostate cancer-related morbidity and mortality. PLOD2 is a mediator of invasion and metastasis that we identified as being upregulated in our highly aggressive radiorecurrent prostate cancer cell line.

METHODS: Patient dataset analysis was conducted using a variety of prostate cancer cohorts. Prostate cancer cell lines were treated with siRNA, or the drug PX-478 prior to in vitro invasion, migration, or in vivo chick embryo (CAM) extravasation assay. Protein levels were detected by western blot. For RNA analysis, RNA sequencing was conducted on PLOD2 knockdown cells and validated by qRT-PCR.

RESULTS: PLOD2 is a negative prognostic factor associated with biochemical relapse, driving invasion, migration, and extravasation in radiorecurrent prostate cancer. Mechanistically, HIF1α upregulation drives PLOD2 expression in our radiorecurrent prostate cancer cells, which is effectively inhibited by HIF1α inhibitor PX-478 to reduce invasion, migration, and extravasation. Finally, the long non-coding RNA LNCSRLR acts as a promoter of invasion downstream of PLOD2.

CONCLUSIONS: Together, our results demonstrate for the first time the role of PLOD2 in radiorecurrent prostate cancer invasiveness, and point towards its potential as a therapeutic target to reduce metastasis and improve survival outcomes in prostate cancer patients.

BJC Reports; https://doi.org/10.1038/s44276-024-00085-3

INTRODUCTION

Prostate cancer (PCa) is the second most prevalent cancer in men worldwide, with over a million cases being diagnosed every year [1–3]. External beam radiation therapy is a primary treatment modality for localized PCa. However, over half of high-risk patients will experience biochemical relapse (BCR) signaling a recurrence of their cancer (radiorecurrent PCa) –the majority of which will develop metastatic disease within ten years [4]. Metastatic PCa is a devastating disease that remains incurable despite advances in systemic therapy [5]. With a 5-year survival rate as low as 30% [6, 7], metastatic PCa emerges as a leading cause of cancer-related mortality in men worldwide [8].

Metastasis is a lethal development in human cancers [9] that is generally conceptualized through five key steps: local invasion of tumor cells from the primary site into the surrounding tissue; intravasation into nearby lymphatic or blood vessels; transit through the circulation; and subsequent extravasation from the vasculature to initiate the final step of colonization and growth in a distant organ [10]. These five phases of metastasis, termed the "metastatic cascade", offer several fronts at which the metastatic dissemination of cancer may be further investigated. There are multiple mechanisms by which cancer cells adopt a metastatic phenotype; cellular reprogramming such as epithelial to mesenchymal transition (EMT) can alter adhesion and motility of cells [11], while the dysregulation of genes involved in collagen remodeling have gained recent attention as a means by which cancer cells promote survival in and invasion through the extracellular matrix (ECM) [12].

The mechanisms by which radiorecurrent cancer acquires heightened metastatic propensity are poorly understood [13]. To explore this phenomenon, our group previously generated radiorecurrent DU145 PCa cells (DU145-CF), which in addition to being more radiation-resistant than their treatment-naïve parental cells (DU145-PAR), are also significantly more invasive [14]. Subsequent proteomic analysis [15] comparing the two cell lines revealed thousands of dysregulated proteins, including the upregulation of procollagen-lysine 2-oxoglutarate 5-dioxygenase 2 (PLOD2) in the DU145-CF cells. The PLOD2 gene encodes the protein lysyl hydroxylase 2 (LH2), an enzyme that hydroxylates the lysine residues of collagen precursor molecules in the endoplasmic reticulum. Outside of the cell, these hydroxyl residues are converted to aldehydes by lysyl oxidases (LOXs), then undergo further reactions that crosslink the collagen molecules. The fibrillar collagen structures formed by these reactions ultimately

[1]Department of Medical Biophysics, University of Toronto, Toronto, ON, Canada. [2]Sunnybrook Research Institute, Sunnybrook Health Sciences Centre, Toronto, ON, Canada. [3]University of California Los Angeles, Los Angeles, CA, USA. [4]Department of Medicine, University of Toronto, Toronto, ON, Canada. [5]Department of Laboratory Medicine and Pathobiology, University of Toronto, Toronto, ON, Canada. [6]Princess Margaret Cancer Centre, University Health Network, Toronto, ON, Canada. [7]Department of Radiation Oncology, University of Toronto, Toronto, ON, Canada. ✉email: stanley.liu@sunnybrook.ca

Received: 19 March 2024 Revised: 23 July 2024 Accepted: 27 July 2024
Published online: 21 August 2024

constitute the major structural component of the ECM [16]. Within the context of cancer progression, PLOD2 has been reported to remodel the collagen around tumors and enhance cell motility; as a result, it is implicated as a driver of invasion, migration, and metastasis in numerous different cancers such as undifferentiated pleomorphic sarcoma [17], non-small cell lung cancer [18], and cervical cancer [19], among others [20–24].

Herein, we identified PLOD2 as a negative prognostic factor driving invasion and metastatic propensity in radiorecurrent PCa. Notably, we demonstrated that PLOD2 promotes extravasation in our DU145-CF cell line. Mechanistic investigations revealed HIF1α as a key regulator of PLOD2 expression upregulated in our DU145-CF cells. Treatment of DU145-CF cells with HIF1α inhibitor PX-478 reduced both HIF1α and PLOD2 protein expression, and significantly attenuated invasion, migration, and extravasation, thereby exhibiting potential as a targeted therapy against PLOD2 to reduce metastasis. Finally, RNA sequencing of PLOD2 knockdown DU145-CF cells revealed the long non-coding RNA LNCSRLR to be a novel downstream target of PLOD2, involved in promoting the invasive phenotype associated with PLOD2.

MATERIALS AND METHODS

Bioinformatic patient analysis

ICGC PRAD-CA patients with pathologically confirmed prostate cancers were used in this study. Fresh-frozen samples of treatment and hormone naïve tumors were sequenced and processed as described before [25–28]. Patients were treated with either radiotherapy or radical prostatectomy. Following radiotherapy, BCR was defined as an increase of more than 2.0 ng/mL above the nadir serum PSA abundance. Following radical prostatectomy, BCR was defined as two consecutive measurements of more than 0.2 ng/mL after surgery. CNAs were defined as previously described [29] in 380 ICGC patients. A Cox proportional hazard model was used to assess the relationship between PLOD2 amplification and BCR risk, using the survival R package v3.2-10. ICGC PRAD-CA CNA data is made available in a previous publication [29].

RNA sequencing was performed as previously described in 140 ICGC patients who received radical prostatectomy treatment [27], and transformed transcript per million (TPM) RNA values were used. Spearman correlations were calculated to evaluate the relationship between PLOD2 and LNCSRLR RNA abundances. Visualizations and statistical analysis were conducted in the R statistical environment v4.2.0. Related plots were created using the BPG package v7.0.3 [30]. ICGC PRAD-CA RNA data is made available in a previous publication [27], and has been deposited in the Gene Expression Omnibus (GEO) under the accession number GEO: GSE84043.

Comparison of PLOD2 RNA expression between localized prostate tumor samples ($n = 65$), and metastatic castrate-resistant prostate cancer (mCRPC) samples ($n = 25$) derived from metastatic sites of 4 patients, was conducted using a dataset accessed from the Gene Expression Omnibus (GEO) under the accession number GEO: GSE6919. RNA was extracted and gene expression was analyzed as previously described [31]. The Student's *t* test was used to assess statistical significance.

Evaluation of PLOD2 RNA expression in benign, localized, and mCRPC patients was performed using data from the Prostate Cancer Transcriptome Atlas (PCTA; http://www.thepcta.org/), an online database comprised of 1321 clinical specimens computationally assembled from 38 distinct cohorts [32]. The One-way ANOVA test was used to assess statistical significance between subsets.

The Cancer Genome Atlas (TCGA) prostate cohort comprises samples from 333 primary prostate carcinomas [33], and was downloaded from the cBioPortal website (https://www.cbioportal.org) to assess PLOD2-HIF1α RNA-RNA correlation. Spearman correlations were calculated to assess the relationship between PLOD2 and HIFα mRNA expression (RNA Seq V2 RSEM).

Cell culture

The human prostate adenocarcinoma cell lines DU145, PC3, and 22RV1 were purchased from the American Type Culture Collection (ATCC), and tested negative for mycoplasma contamination. The DU145-CF cell line was generated as previously described [14]. Cells were grown on tissue-culture flasks in Dulbecco's modified Eagle's medium containing 4.5 g/L D-glucose and GlutaMAX (DMEM; Gibco, USA) supplemented with 10% Fetal Bovine Serum (FBS) and 1% Penicillin-Streptomycin. The cells were kept at 37°C in a humidified incubator with 5% CO2 and passaged upon reaching 80% confluency.

Primary cell derivation and culture

Targeted biopsy core sample was taken from the primary tumor (Gleason 7) at time of brachytherapy treatment and immediately transported to the laboratory. Sample was washed with PBS, finely minced, then digested overnight in collagenase I solution (Worthington Biochemical). The following day, the biopsy was further trypsin digested, and cells were ultimately plated on a collagen-coated 10 cm dish (Corning) in human prostate culture media for derivation [34]. Cells tested negative for mycoplasma contamination.

siRNA transfection

To knockdown PLOD2 expression in the experimental cell lines, cells were seeded in 6-well plates and transfected with scramble control (CAT#: SR30004; Origene Inc., USA) or PLOD2 siRNA (CAT#: SR321350; Origene Inc., USA) using siTran 2.0 Transfection Reagent (CAT#: TT320001; Origene Inc., USA). Cells were assayed 24 hours after transfection. To knockdown LNCSRLR expression, the same protocol was implemented using LNCSRLR siRNA from Invitrogen using the previously published sequence: 5′-GUUACUGUACAUCAGGAAUTT-3′ [35].

PX-478 treatment

Experimental cell lines were seeded in 6-well plates and left to incubate overnight, then treated with H_2O control or 20 μM PX-478 (Catalog No. S7612; Selleckchem) reconstituted in H_2O. Cells were assayed 24 h after treatment.

Clonogenic survival assay

Scramble control and PLOD2 siRNA-transfected cells were plated in triplicate on 6-well plates and mock-irradiated at 0 Gy or irradiated with 4, 6, and 8 Gy, then incubated at 37 °C in a humidified incubator with 5% CO_2. After 14 days, the cells were stained with crystal violet (Sigma) and colonies of >50 cells were counted. Surviving fraction of each cell line was determined by dividing the plating efficiency of irradiated cells by the plating efficiency of mock-irradiated cells. The surviving fraction data was fitted to the linear quadratic formula $s = e^{-\alpha D - \beta D2}$ to produce a dose-response curve.

Proliferation assay

Cells transfected with scramble control or PLOD2 siRNA were seeded at a density of 0.5×10^5 cells per well in triplicate. After 5 days of incubation, cells were trypsinized and viable cells were counted using trypan blue dye exclusion on the Countess automated cell counter (Invitrogen, USA). Fold change in proliferation was calculated by normalizing treated cell count to control cell count.

Transwell invasion and migration assays

Cells were serum-starved in FBS-free DMEM and seeded in the upper chamber of 8μm-pore transwell inserts (Corning, USA) precoated with 1 mg/ml Matrigel (Corning, USA) for invasion assays, or uncoated for migration assays; DMEM supplemented with 10% FBS was added to the lower chamber as a chemoattractant. After 24 hours, cells that invaded or migrated through the transwell membrane were fixed and stained using the Kwik-Diff Stain kit (Thermo Fisher Scientific, USA). Quantification of cells was achieved by counting the number of invaded or migrated cells on the transwell imaged at ×4 magnification using the BioTek Cytation 5 Cell Imaging Multimode Reader (Agilent, USA).

CAM assay

The chicken CAM assay was performed as previously described [36]. DU145-CF cells stably expressing GFP were transfected or drug-treated in 6-well plates. Upon growing to 80–90% confluency 24 h post-treatment, cells were resuspended in phosphate-buffered saline (PBS) (Wisent, Canada) at a concentration of 5×10^5 cells/ml; 100 μl of either control or treated DU145 cells were injected into randomly selected CAMs of day 13 embryos via microinjector ($n > 5$ per group). Intravascular cells were counted at $T = 0$ h in a region of interest (ROI) demarcated by a 0.5×0.5-

inch aluminum foil window, and extravasated cells were counted in the same ROI at T = 24 h. The extravasation efficiency of each embryo was calculated by dividing the number of extravasated cells at T = 24 h by the number of initial intravascular cells at T = 0 h within the ROI. Mean extravasation efficiencies were calculated using extravasation efficiencies of individual control or treatment embryos.

Western blotting

To assess protein reduction by siRNA knockdown, cells were transfected with siRNA and lysed after 48 h. For protein detection after PX-478 treatment, cells were treated for 24 h then lysed. For protein detection of untreated cell lines, cells were lysed 24 h after seeding. Cells were lysed using RIPA lysis buffer mixed with Complete Mini protease inhibitor cocktail and PhosSTOP phosphatase inhibitor cocktail (Roche Diagnostics, USA). Lysates were separated on a 4-20% polyacrylamide gel (Bio-Rad, USA), and wet transferred to a polyvinylidene difluoride (PVDF) membrane (Thermo-Fisher Scientific, USA). Membranes were blocked with 5% bovine serum albumin (BSA) in Tris-Buffered Saline Tween-20 (TBST) and incubated overnight at 4 °C with primary antibody. The next day, membranes were incubated at room temperature with horseradish peroxidase-conjugated secondary antibody (1:5000 dilution) for 1 hour. PLOD2 protein was detected using PLOD2 antibody (1:1000 dilution) (Cat. # 44709 S; Cell Signaling Technology, USA), and β-actin was detected as a loading control using β-actin antibody (1:2000 dilution) (Cat. # 4967 S; Cell Signaling Technology, USA). HIF1α protein was detected using HIF1α antibody (1:1000 dilution) (Cat. # 36169 S; Cell signaling Technology, USA). Blots were imaged using ECL substrate (Bio-Rad, USA) on the ChemiDoc Imaging System (BioRad, USA).

Quantitative real-time PCR (qRT-PCR)

Quantification of RNA expression was done by extracting total RNA from cells using RNeasy Mini Kit (Qiagen, USA), which was then converted to cDNA for amplification using SuperScript VILO Master Mix (Thermo-Fisher Scientific). TaqMan Fast Advanced Master Mix (Thermo-Fisher Scientific, USA) was combined with cDNA and predesigned Taqman Gene Expression Assay primers for PLOD2 (Assay ID: Hs01118200; Thermo-Fisher Scientific, USA) and GAPDH (Assay ID: Hs99999905, Thermo-Fisher Scientific, USA) to initiate the qRT-PCR. For quantification of LNCSRLR expression, Power Up SYBR Green Master Mix (Thermo-Fisher Scientific, USA) was combined with cDNA and SYBR Green primers from Thermo-Fisher Scientific using the previously published sequence: (FW: 5′-CACTGTTCCAGGCACCAAGG-3′) (RV: 5′-TGTCGCCAAAGAAGAGAACAGG-3′) [35]. RNA expression was determined by comparative Ct method using QuantStudio 3 Design and Analysis Software (Thermo-Fisher Scientific, USA). GAPDH was used as an endogenous control to assess relative levels of the RNA of interest within each cell line.

RNA sequencing analysis

Samples for sequencing were prepared by extracting total RNA from DU145-CF cells transfected with scramble control or PLOD2 siRNA using RNeasy Mini Kit (Qiagen, USA). RNA library preparation, sequencing, and bioinformatic analysis was performed by Novogene Co., LTD. (Sacramento, USA).

Statistical analysis

All statistical analysis was performed with GraphPad Prism 10.0 (GraphPad Software Inc., USA). The Student's *t* test was used to assess difference in mean values between two groups, with significance defined as $P < 0.05$ (*$p < 0.05$; **$p < 0.01$; ***$p < 0.001$; ****$p < 0.0001$). Unless otherwise stated, all data is presented as mean values with standard deviation.

RESULTS

PLOD2 is overexpressed in radiorecurrent prostate cancer cells and associated with biochemical relapse and metastatic disease

To generate the radiorecurrent DU145-CF cell line, we previously treated DU145 cells with a daily 2 Gy fraction of ionizing radiation over several weeks, to simulate the clinical scenario of resistance to conventional fractionation [14]. Proteomic analysis was conducted on DU145-CF cell lysates, which identified PLOD2 as an upregulated protein involved in pathways previously implicated with radiation resistance [15]. To investigate PLOD2 as a potential driver of radiorecurrent PCa metastasis, we first sought to validate the results of the proteomic analysis. By western blot, we confirmed that PLOD2 protein is upregulated in our radiorecurrent DU145-CF cells compared to DU145-PAR cells (Fig. 1a). Since PLOD2 has been associated with poor survival outcomes in other cancers [24, 37], we analyzed the data of 380 PCa patients from the ICGC PRAD-CA (CPC-GENE) study, which revealed PLOD2 genomic amplification to be significantly associated with reduced BCR-free survival time (Fig. 1b). A positive association of PLOD2 expression was also seen in metastatic disease (Fig. 1c, d). Together, this data suggests that PLOD2 is a negative prognostic factor in PCa, and may be involved in driving aggressive phenotypes.

PLOD2 drives invasion and migration in prostate cancer in vitro

We performed radiation clonogenic survival assays to test whether PLOD2 conferred resistance to radiation. However, knockdown of PLOD2 with siRNA in DU145-CF and DU145-PAR cells did not alter sensitivity to radiation (Supplementary Fig. 1A, B). DU145-CF cells possess enhanced proliferative capacity [14], however PLOD2 knockdown in DU145-CF and -PAR cells had no effect on proliferation (Supplementary Fig. 2A, B).

To assess whether PLOD2 contributes to the aggressive metastatic phenotype observed in our radiorecurrent cells [14], we conducted Matrigel invasion assays. Consistent with previous studies implicating PLOD2 in invasion [19, 22, 23], knockdown of PLOD2 by siRNA significantly reduced invasion in our radiorecurrent DU145-CF cells (Fig. 2a). PLOD2 knockdown also suppressed invasion in DU145-PAR, PC3, and 22RV1 PCa cells (Fig. 2b–d). Further, PLOD2 knockdown significantly reduced invasion in a primary PCa cell line derived from the biopsy of a patient with intermediate (Gleason 7) PCa (Fig. 2e). Validation of siRNA-mediated PLOD2 knockdown in each cell line was confirmed by western blot (Supplementary Fig. 3).

As PLOD2 is a collagen-modifying enzyme, it may enhance invasion by interacting with collagen present in Matrigel [38]; we therefore conducted transwell migration assays without Matrigel to investigate whether PLOD2 can promote cell-intrinsic motility in the absence of external collagen barriers. PLOD2 knockdown significantly reduced migratory capacity in DU145-CF, DU145-PAR, and 22RV1 PCa cell lines (Fig. 2f, g, i). A strong trend towards reduction in migration was observed with PLOD2 knockdown in the primary 107-I7 cell line, although non-significant (Fig. 2j). Surprisingly, PLOD2 knockdown had no effect on migration in PC3 cells (Fig. 2h), suggesting the existence of distinct mechanisms by which PLOD2 promotes either invasion or migration, that may vary between cell lines. In summary, these findings reveal that PLOD2 promotes invasion and migration in radiorecurrent PCa and numerous other PCa cell lines, including a primary cell line. These results also suggest a role for PLOD2 in promoting invasion in vivo.

PLOD2 promotes extravasation of radiorecurrent prostate cancer in vivo

Extravasation is a critical step in the metastatic cascade required for cancer cells to exit the circulation and colonize distant organs [10]. PLOD2 has been speculated to be involved in extravasation as a known mediator of metastatic dissemination [17]. However, investigation of the role of PLOD2 in extravasation has been limited to date. To this end, we employed the chorioallantoic membrane (CAM) assay, a validated method of evaluating invasion in vivo by quantifying cancer cell extravasation from the CAM vasculature into the surrounding stroma [36]. GFP-labeled DU145-CF cells transfected with control or PLOD2 siRNA were injected into CAM embryos and allowed to extravasate over

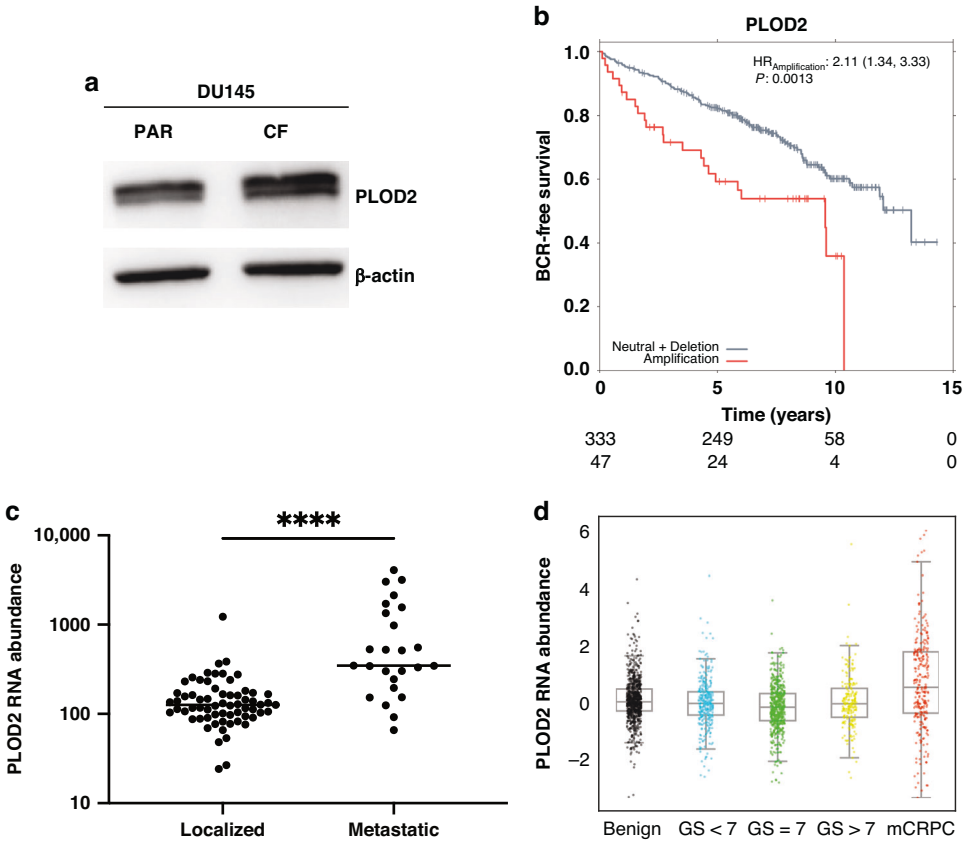

Fig. 1 PLOD2 is overexpressed in radiorecurrent prostate cancer cells and associated with biochemical relapse and metastatic disease. **a** Representative western blot of PLOD2 protein levels in DU145-PAR and DU145-CF cells; β-actin used as loading control. **b** Kaplan-Meier plot of biochemical relapse (BCR)-free survival rate for ICGC PRAD-CA patients with PLOD2 amplification versus neutral+deletion copy number alteration ($n = 380$). **c** Comparison of PLOD2 RNA expression in localized prostate tumor samples ($n = 65$) and metastatic castrate-resistant prostate cancer (mCRPC) samples ($n = 25$) derived from metastatic sites of 4 patients (****$P < 0.0001$). Data retrieved from the Gene Expression Omnibus (GEO) dataset GSE6919. **d** Comparison of PLOD2 RNA expression in benign, localized, and mCRPC patients ($n = 1321$; One-way ANOVA test between subsets: F-value = 11.147, $P < 0.001$). Data derived from the Prostate Cancer Transcriptome Atlas (PCTA).

a 24-hour period (Fig. 3a). Corroborating our previous invasion and migration results, PLOD2 knockdown in our radiorecurrent DU145-CF cells resulted in an approximate 50% reduction in extravasation efficiency (Fig. 3b). Collectively, these results directly implicate PLOD2 as a driver of extravasation and overall metastatic potential in radiorecurrent PCa, warranting investigation of targetable upstream pathways driving PLOD2 expression.

PX-478 suppresses PLOD2 expression through HIF1α inhibition

It is well-established that PLOD2 is upregulated in hypoxic conditions by hypoxia-inducible factor-1α (HIF1α) [17, 19, 21, 24, 37, 39]. Therefore, we investigated the relationship between PLOD2 and HIF1α in the PCa patient cohort of The Cancer Genome Atlas (TCGA) database [33], which revealed a significant positive association in RNA expression between these two targets (Fig. 4a). Our prior proteomic analysis indicated enrichment in hypoxic signaling in DU145-CF cells relative to DU145-PAR cells [15]. Strikingly, western blot analysis revealed greatly increased HIF1α protein in DU145-CF cells compared to DU145-PAR under normoxic conditions, which corresponded to elevated PLOD2 levels (Fig. 4b). To confirm that PLOD2 expression was regulated by hypoxic signaling in our radiorecurrent cells, we incubated DU145-CF cells under hypoxic conditions (1% O_2) overnight. We observed a further increase in PLOD2 protein under hypoxic conditions, concomitant with intense increase of HIF1α (Fig. 4c).

Next, we explored the possibility of suppressing PLOD2 expression with a HIF1α inhibitor. To test this hypothesis, we treated DU145-PAR and DU145-CF cells with 20 μM of the validated HIF1α inhibitor PX-478 [40, 41] for 24 h under normoxic conditions, which substantially inhibited the expression of both HIF1α and PLOD2 in the two cell lines (Fig. 4d, e). Following this, we examined whether PX-478 could maintain its inhibitory effects on HIF1α and PLOD2 in hypoxic cells; DU145-CF cells were therefore treated with 20 μM of PX-478 and incubated under hypoxic conditions overnight. Despite high levels of HIF1α and PLOD2 protein in response to hypoxia, PX-478 retained its ability to inhibit expression of both proteins, by approximately 25% (Supplementary Fig. 4A–C). In summary, we have identified HIF1α as an upstream driver of elevated PLOD2 expression in our DU145-CF cells, and as a result, attenuation of both HIF1α and PLOD2 protein expression was achieved through treatment with HIF1α inhibitor PX-478. These results therefore suggest a potential function of PX-478 in suppressing the metastatic phenotype of radiorecurrent PCa.

PX-478 treatment reduces invasion, migration, and extravasation in radiorecurrent prostate cancer

To investigate the prospect of administering PX-478 as an anti-metastatic therapy against PLOD2 in radiorecurrent PCa, we treated DU145-CF cells with 20 μM of PX-478 for 24 h before evaluating their invasion and migration. Although no effect on cell viability was observed at this concentration (Supplementary Fig. 5), 20 μM of PX-478 significantly reduced in vitro invasion and

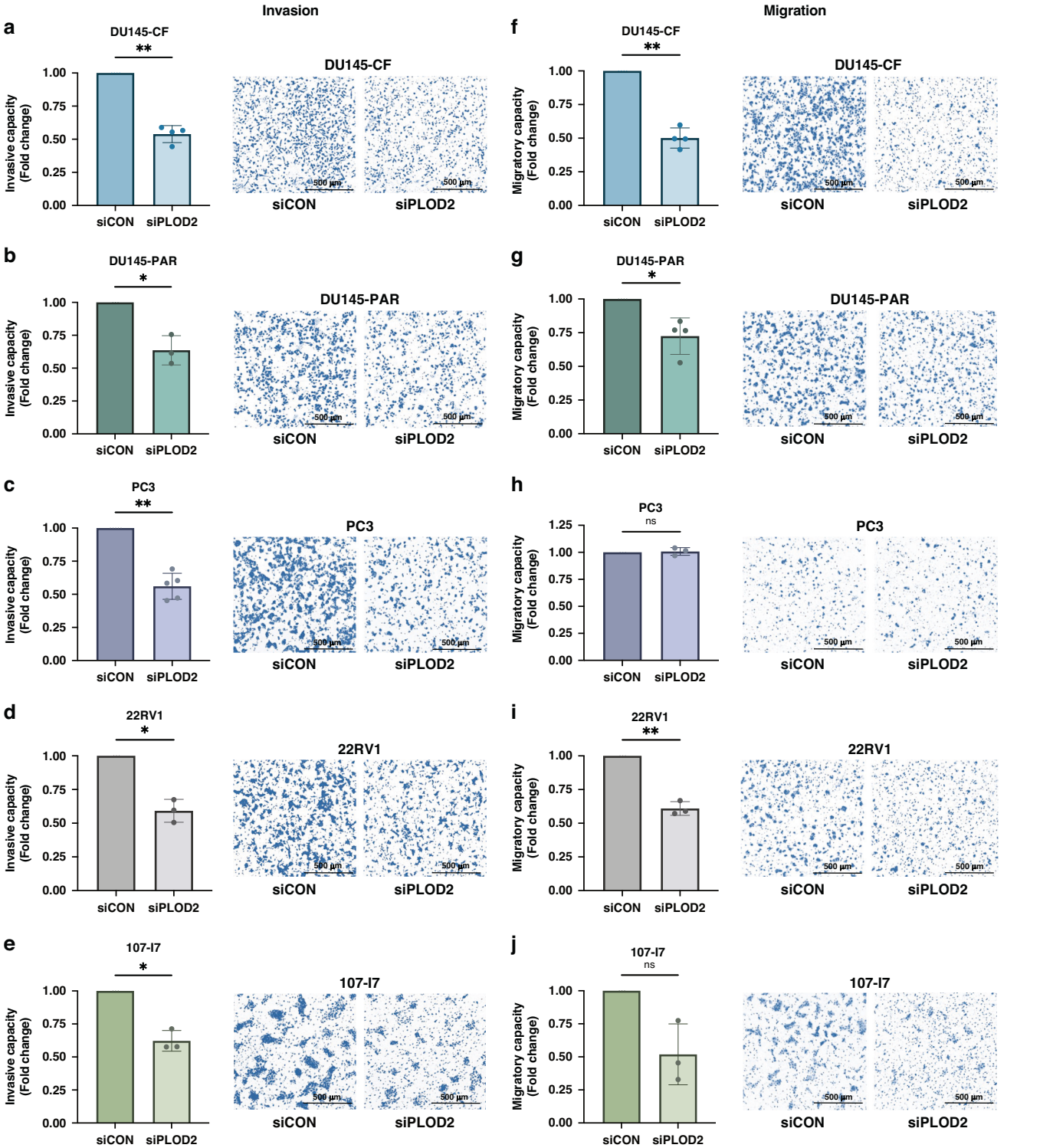

Fig. 2 PLOD2 drives invasion and migration in prostate cancer in vitro. Matrigel-coated transwell invasion assays were conducted with numerous PCa cell lines transfected with scramble control (siCON) or PLOD2 (siPLOD2) siRNA: (**a**) DU145-CF; (**b**) DU145-PAR; (**c**) PC3; (**d**) 22RV1; (**e**) 107-I7 primary line. Transwell migration assays were repeated for each cell line: (**f**) DU145-CF; (**g**) DU145-PAR; (**h**) PC3; (**i**) 22RV1; (**j**) 107-I7 primary line. Means, standard deviations, and statistical significance of biological replicates are shown (ns = not significant, $^{*}P < 0.05$, $^{**}P < 0.01$).

migration in DU145-CF cells (Fig. 5a, b). Similar results were obtained in PX-478-treated DU145-PAR cells (Supplementary Fig. 6). To assess its ability to decrease in vivo invasion, DU145-CF cells were treated with 20 µM of PX-478 24 h prior to injection into CAM embryos. Consistent with its inhibitory effects on invasion and migration, PX-478 significantly diminished extravasation in DU145-CF cells (Fig. 5c). Overall, these results demonstrate the potential of PX-478 as a pharmacological therapy to abrogate invasion, migration, and extravasation in radiorecurrent PCa. These findings therefore prompted us to further consider the

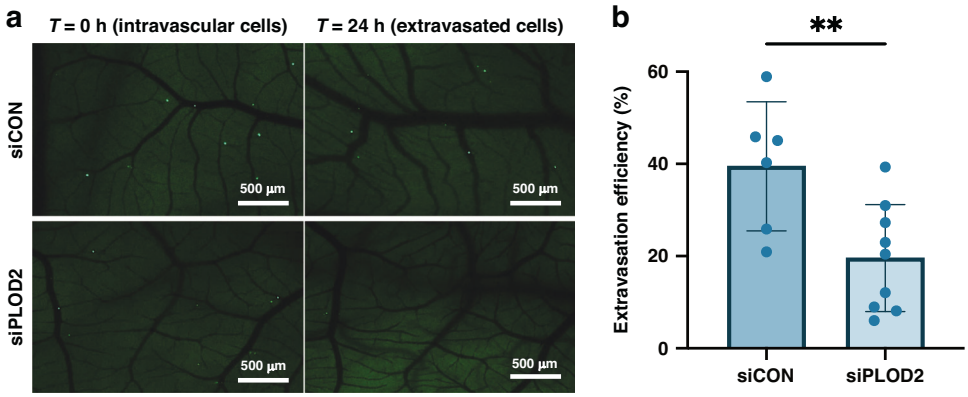

Fig. 3 PLOD2 promotes extravasation of radiorecurrent prostate cancer in vivo. a Representative images of ROIs on CAM embryos injected with scramble control siRNA-treated DU145-CF cells (siCON) or PLOD2 siRNA-treated DU145-CF cells (siPLOD2), at time = 0 h (intravascular cells) and time = 24 h (extravasated cells); Bright green foci: GFP-labeled DU145-CF cells; Dark green background: CAM stroma; Black: CAM blood vessels. Images were taken with a fluorescence microscope. **b** Extravasation efficiency of DU145-CF cells transfected with scramble control siRNA (siCON) or PLOD2 siRNA (siPLOD2), calculated from surviving embryos 24 h post-cell injection. Means, standard deviations, and statistical significance of biological replicates are shown (**$P < 0.01$).

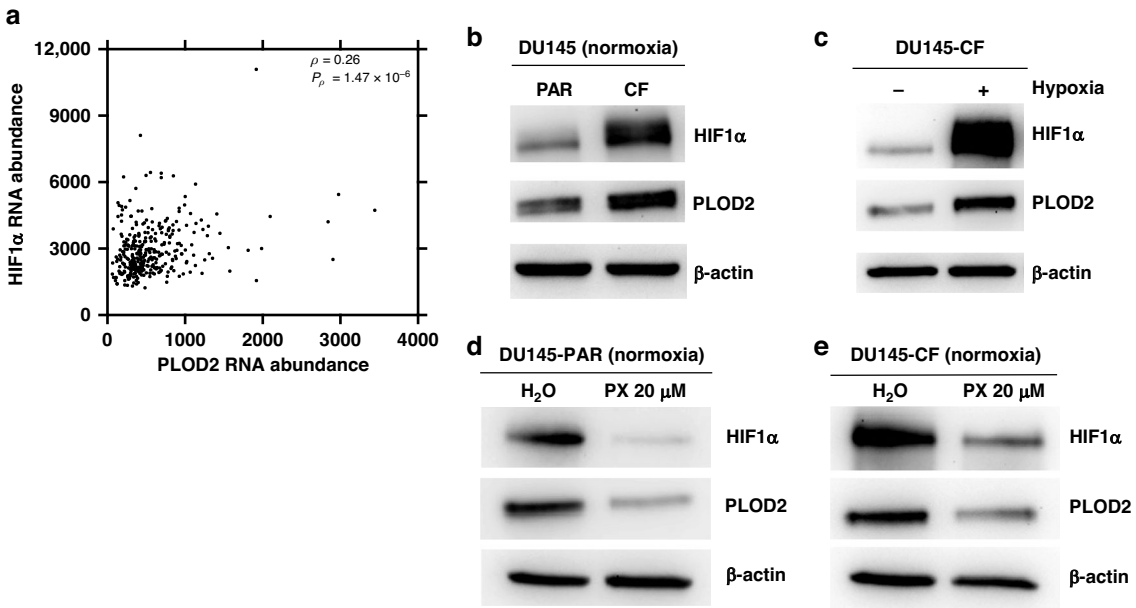

Fig. 4 PX-478 suppresses PLOD2 expression through HIF1α inhibition. a Spearman correlation test of PLOD2 and HIF1α RNA expression in the PCa cohort of TCGA ($n = 333$). **b** Western blot of HIF1α and PLOD2 protein levels in DU145-PAR (left) and DU145-CF (right) cell lysates. **c** Western blot of HIF1α and PLOD2 protein levels in DU145-CF cell lysates under normoxic (left) and hypoxic (right) conditions. For hypoxic conditions, DU145-CF cells were left incubated at 1% O_2 for 16 h. Western blots of HIF1α and PLOD2 protein levels in DU145-PAR cells (**d**) and DU145-CF cells (**e**) treated with H_2O control or 20 µM of PX-478 (PX) for 24 h. β-actin was used in all western blots as a loading control.

cellular mechanisms downstream of PLOD2 that are suppressed by PX-478.

PLOD2 promotes invasion through upregulation of LNCSRLR

It has previously been shown that PLOD2 promotes metastasis via ECM remodeling in vivo as a procollagen-modifying enzyme [42–45]. However, our in vitro transwell assays indicated that PLOD2 can modulate cell motility independently of its interaction with extracellular collagen; this suggests alternative mechanisms by which PLOD2 regulates these dynamics. To investigate whether PLOD2 is involved in the regulation of additional genes promoting cell motility, we conducted RNA-sequencing on DU145-CF cells transfected with PLOD2 siRNA and compared their gene expression to control siRNA-treated samples. Knockdown of PLOD2 caused widespread changes in transcriptional expression and significant dysregulation of multiple pathways (Supplementary Fig. 7). After false discovery rate (FDR) correction, 11 genes were found to be significantly dysregulated, with the most down-regulated (11.8-fold) being LNCSRLR (Fig. 6a). Sorafenib Resistance In Renal Cell Carcinoma Associated (LNCSRLR) is a novel long non-coding RNA first characterized in 2016 [46]. Although the full extent of its cellular mechanisms remains largely unknown, LNCSRLR has been previously identified as a promoter of invasion and migration in hepatocellular carcinoma [35]; therefore, we selected this gene candidate for further investigation. To validate the results of the RNA sequencing, we assessed the expression levels of both PLOD2 and LNCSRLR in our PLOD2-knockdown DU145-CF cells by qRT-PCR, which confirmed significant down-regulation of PLOD2 expression (Fig. 6b) and a corresponding decrease in LNCSRLR expression (Fig. 6c). We examined the association between these two genes in treatment-naïve PCa patients receiving radical prostatectomy from the ICGC PRAD-CA

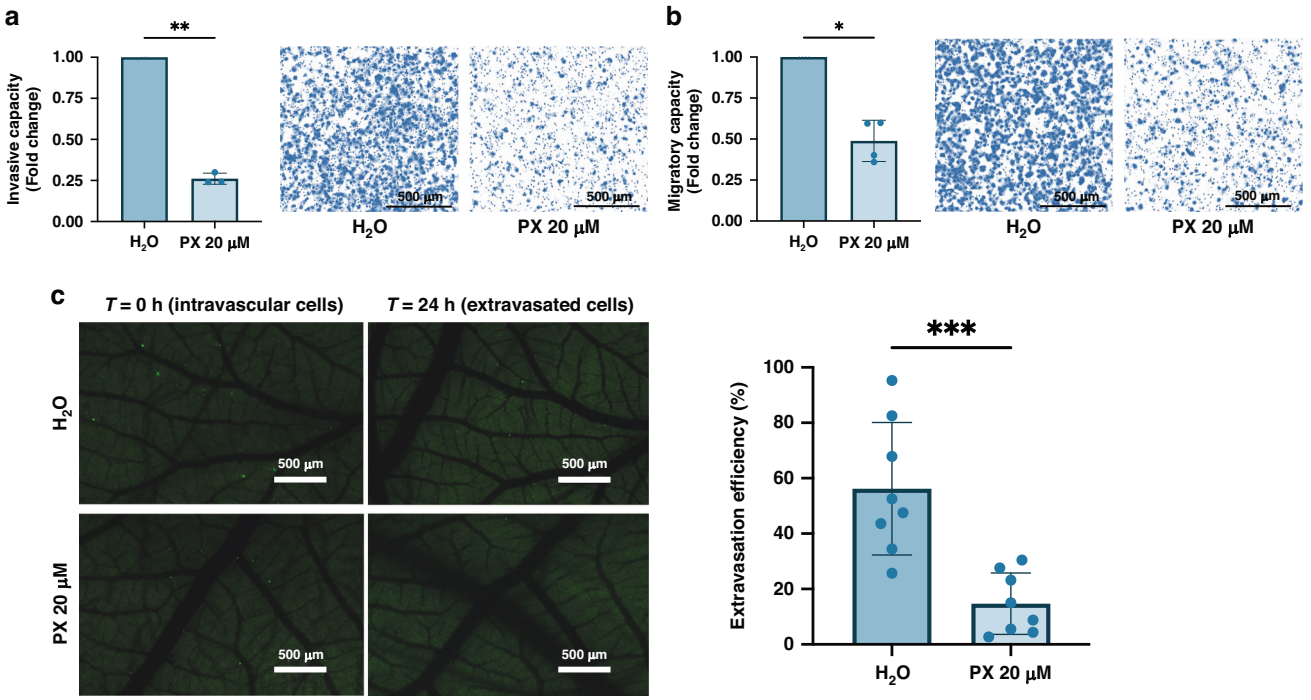

Fig. 5 PX-478 treatment reduces invasion, migration, and extravasation in radiorecurrent prostate cancer. Matrigel-coated transwell invasion assay (**a**), transwell migration assay (**b**), and CAM extravasation assay (**c**) of DU145-CF cells treated with H_2O control or 20 µM PX-478 (PX) for 24 h prior to assay. Means, standard deviations, and statistical significance of biological replicates are shown (*$P < 0.05$, **$P < 0.01$, ***$P < 0.001$).

database, which revealed a remarkably significant positive association between PLOD2 and LNCSRLR RNA expression in the clinical context (Fig. 6d).

To functionally validate LNCSRLR as a pro-metastatic gene, we performed LNCSRLR knockdown in our DU145-CF cells (Fig. 6e) and assessed their invasive and migratory capacity. LNCSRLR knockdown significantly reduced invasion in our DU145-CF cells (Fig. 6f); migration was slightly reduced but not significantly (Supplementary fig. 8). Furthermore, treatment of DU145-CF cells with 20 µM of PX-478 significantly reduced LNCSRLR expression (Fig. 6g), implicating LNCSRLR as a downstream mediator of invasion in the HIFα-PLOD2 regulatory axis. To summarize these findings, we have identified a novel relationship between PLOD2 and LNCSRLR, whereby the expression of the pro-invasive LNCSRLR is driven by PLOD2; therefore, LNCSRLR upregulation acts as one mechanism by which PLOD2 induces a metastatic phenotype in radiorecurrent PCa.

DISCUSSION

The molecular factors conferring metastatic potential in radiorecurrent prostate cancer remain understudied, despite the critical need for new therapeutic modalities that target the progression of radiorecurrent metastasis. We identified PLOD2 as a negative prognostic factor associated with biochemical relapse in prostate cancer patients, that is overexpressed in our radiorecurrent prostate cancer cell line DU145-CF. We revealed that PLOD2 contributes to the aggressive metastatic phenotype of DU145-CF cells by promoting in vitro invasion, migration, and in vivo extravasation; these metastatic mechanisms were effectively inhibited by PX-478, a pharmacological agent that suppresses PLOD2 expression through its upstream mediator HIF1α. Mechanistically, we demonstrated that the metastatic phenotype of PLOD2 is driven in part by the pro-invasive long non-coding RNA LNCSRLR, whose expression is promoted by PLOD2. We hereby present a novel HIF1α-PLOD2-LNCSRLR regulatory axis that confers an invasive phenotype in radiorecurrent prostate cancer. Since knockdown of PLOD2 did not influence intrinsic radiosensitivity, as determined by radiation clonogenic assay, it is unlikely that PLOD2 contributes to the development of radiorecurrence. Instead, we propose that PLOD2 upregulation serves as a driver of tumor progression following radiorecurrence, namely through promotion of invasion and metastasis. Understanding such mechanisms is a crucial first step in expanding the limited therapeutic options currently available to suppress the aggressive clinical progression of radiorecurrent prostate cancer.

One of the first comprehensive investigations into the role of PLOD2 in cancer progression revealed its function as a critical driver of migration and metastasis under hypoxic conditions in undifferentiated pleomorphic sarcoma (UPS) [17]. It has since been identified to promote invasion, migration, and metastasis in a diversity of cancer types including carcinomas [18–24], gliomas [39] and other sarcomas [47]. To our knowledge, we report for the first time that PLOD2 promotes metastatic progression in prostate cancer, and particularly in radiorecurrent prostate cancer. PLOD2 knockdown not only decreased in vitro invasion in the radiorecurrent DU145-CF cell line, but this effect was also recapitulated in numerous other PCa cell lines including DU145-PAR (radiation-naïve DU145 cells), PC3, and 22RV1. DU145 is an androgen-independent cell line derived from a brain metastasis of prostate adenocarcinoma [48], thereby modeling advanced-stage prostate cancer in its radiation-naïve form (DU145-PAR). The finding that PLOD2 knockdown significantly attenuates invasion in the significantly more aggressive DU145-CF cell line supports its potential utility as a therapeutic target in patients whose advanced prostate cancer has become non-responsive to conventional local and systemic therapies [1]. Indeed, PLOD2 knockdown also reduced the invasive capacity of PC3 and 22RV1, both of which are androgen-independent cell lines considered to model aggressive, advanced stage prostate cancer [49, 50]. Additionally, PLOD2 knockdown consistently reduced migration in every prostate cancer cell line, with the exception of the PC3

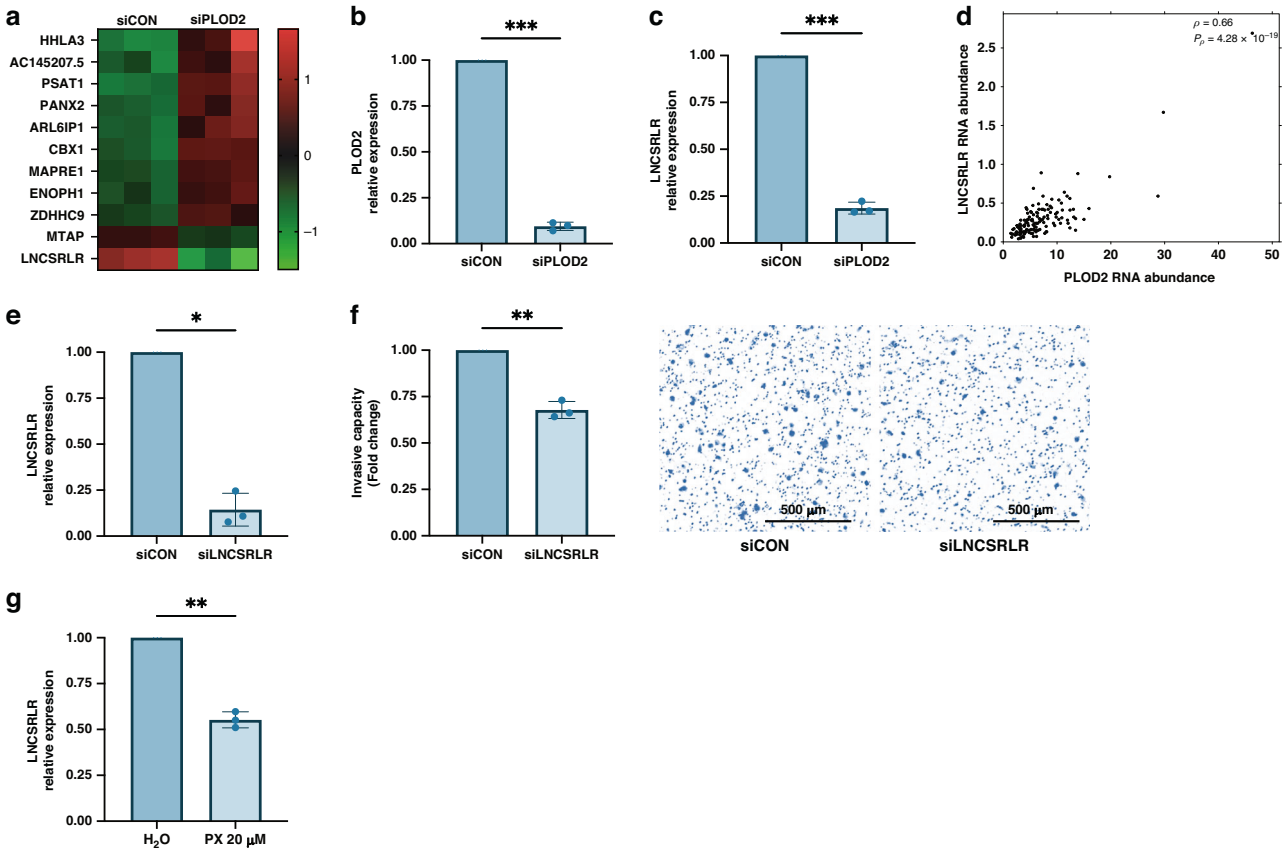

Fig. 6 PLOD2 promotes invasion through upregulation of LNCSRLR. a Heatmap of significantly dysregulated genes in DU145-CF cells transfected with PLOD2 siRNA (siPLOD2) compared to scramble control (siCON), after false discovery rate (FDR) correction (adjusted p-value < 0.05 and |log2(FoldChange)| > 0). PLOD2 (**b**) and LNCSRLR (**c**) RNA expression in DU145-CF cells transfected with PLOD2 siRNA, validated by qRT-PCR (normalized to GAPDH). **d** Spearman correlation test of PLOD2 and LNCSRLR RNA expression in ICGC PRAD-CA patients ($n = 140$). **e** LNCSRLR knockdown with siRNA (siLNCSRLR) validated by qRT-PCR (normalized to GAPDH). **f** Matrigel-coated transwell invasion assay of DU145-CF cells treated with scramble control or LNCSRLR siRNA. **g** qRT-PCR measuring LNCSRLR RNA expression in DU145-CF cells treated with H_2O control or 20 µM of PX-478 (PX) for 24 h. Means, standard deviations, and statistical significance of biological replicates are shown (*$P < 0.05$, **$P < 0.01$, ***$P < 0.001$).

cell line, underscoring its pivotal role in driving cell motility. PC3 is unique among prostate cancer cell lines in that it expresses features of prostatic small cell neuroendocrine carcinoma (SCNC), a rare and aggressive form of prostate cancer that occurs in only 1% of cases [51]. Given that PC3 originates from neuroendocrine carcinoma, it follows that the cell line would be functionally distinct from other prostate adenocarcinoma cell lines. Particularly, the failure to suppress migration by PLOD2 knockdown may suggest the use of additional compensatory mechanisms to maintain cell motility –a response which would be consistent with the uniquely aggressive metastatic phenotype of neuroendocrine prostate cancer.

Much of the characterization of PLOD2 as a metastatic driver has been done in established cell lines modeling aggressive, late-stage disease. However, the paucity of primary cancer cell culture continues to be a critical limitation in the translatability of preclinical research. Primary cell lines retain their heterogeneity while also faithfully recapitulating the genetic and phenotypic profile of the original cancer, thereby providing a more clinically relevant in vitro model to test potential therapeutic avenues [52, 53]. Cognizant of the scarcity in PLOD2 studies using primary cancer cell culture, we also used 107-I7, a primary cell line derived directly from the prostate biopsy of a patient with Gleason 7 (intermediate) castration-sensitive prostate cancer. The reduction in invasion and migration induced by PLOD2 knockdown in 107-I7 cells further supports the therapeutic potential of targeting PLOD2 in prostate cancer. Our findings have also demonstrated the potential utility of PLOD2 as a biomarker for poor prognosis and recurrence in prostate cancer. More broadly, these studies highlight the ubiquity of PLOD2 as a driver of invasion throughout a diverse array of intermediate and advanced prostate cancer cells.

Extravasation is a critical bottleneck in the metastatic cascade where cancer cells in transit exit the hostile circulatory system to establish distant metastatic colonies [10, 54], thereby posing as a promising interface at which to inhibit metastasis. Being a complex process that requires the execution of multiple sequential steps, extravasation provides multiple mechanistic fronts to target: cancer cell adhesion to the endothelial cells lining the lumen of blood vessels; exiting of the blood vessels by transendothelial migration; and invasion through the vascular basement membrane into the adjacent stromal matrix [55]. Since migration and invasion are integral features of this process, PLOD2 has been speculated to promote extravasation [17]. However, its direct impact on extravasation has been scarcely studied, likely due to the difficulty of quantitatively assessing extravasation in a physiologically complex in vivo environment. Using the in vivo CAM model, we demonstrate that PLOD2 knockdown significantly reduces extravasation of radiorecurrent DU145-CF cells. These findings further support its role as a critical driver of invasion in vivo and as a key contributor in multiple stages of the metastatic cascade.

To date, there have been several pathways identified that regulate PLOD2, prominent among these being the Transforming Growth Factor β (TGFβ) [24, 56] and Hypoxia-Inducible Factor (HIF) cell signaling pathways [21, 24, 57]. Initially, we considered the possibility that PLOD2 overexpression in DU145-CF cells was induced through the TGFβ pathway, since their proteomic analysis indicated upregulation of TGFβ-associated proteins [15]. However, subsequent investigations using TGFβ pathway inhibitors did not reduce PLOD2 expression (data not shown). Studies linking PLOD2 expression to upstream hypoxic signaling have been conducted mainly under hypoxic conditions, which led us to doubt that this mechanism of regulation was occurring in our normoxic cells. Despite this, hypoxic signaling was shown to be increased in the proteomic profile of our radiorecurrent cells [15], leading us to the compelling discovery that the HIF1α protein, normally degraded in normoxic conditions [58], was significantly enriched in our DU145-CF cells.

It has been well-established that hypoxia promotes radiation resistance [59]. The presence of oxygen in cells is vital for the permanent fixation of radiation-induced DNA damage that ultimately leads to tumor cell death [60, 61]; therefore, hypoxic conditions can mitigate the effects of radiation-induced DNA damage while also initiating HIF signaling to promote survival of tumor cells [62]. There are nevertheless various non-canonical mechanisms by which HIF signaling is activated independently of low cell oxygenation [63]. In fact, it has previously been shown that HIF signaling can be upregulated in response to radiation-induced reactive oxygen species (ROS) coinciding with tumor reoxygenation [64]. This finding provides one mechanistic proof-of-concept by which radiation treatment could increase HIF1α expression in an oxygenated environment. In addition to PLOD2, HIF signaling induces the expression of numerous other proteins involved in ECM-remodeling and cell motility [13, 62]; with this in mind, it is reasonable to infer that the aggressive metastatic phenotype associated with our DU145-CF cells is in part conferred by active HIF signaling resulting from repeated radiation exposure. Future studies using other radiorecurrent cell lines are needed to further explore the relationship between HIF1α, PLOD2, and radiorecurrent metastasis.

With PLOD2 consistently demonstrating its promise as a therapeutic target in multiple cancer models, there is significant interest in the discovery of inhibitory compounds [65]. A common compound used to inhibit PLOD2 preclinically is minoxidil [17, 21, 24, 66], however treatment with minoxidil did not reduce invasion or PLOD2 protein expression in our cell lines (data not shown), suggesting an alternate mechanism of regulation. PX-478 is a well-validated inhibitor of HIF1α derived from the alkylating agent melphalan –an approved chemotherapy in the treatment of cancers such as multiple myeloma and ovarian adenocarcinoma [67]– and is considered to be selective for HIF1α through its multiple levels of inhibition at the transcriptional, translational, and ubiquitination levels [40]. Treatment with PX-478 is known to reduce HIF1α protein expression in DU145 cells, leading to radiosensitization [41], and has previously been shown to reduce PLOD2 protein expression in glioma cells [39]. Here we have demonstrated that inhibition of PLOD2 by PX-478 also reduces invasion, migration, and extravasation. PX-478 treatment has been reported to mediate various biological effects such as reducing cell proliferation and promoting apoptosis in vitro while suppressing tumor growth in vivo [68, 69]; nevertheless, HIF1α is known to influence multiple hallmarks of cancer, and thus these effects are generally considered as being direct results of HIF1α inhibition. Our findings therefore highlight PX-478 as a potential therapeutic inhibitor of HIF1α-driven PLOD2 and radiorecurrent metastasis. Despite limited progress in the clinical development of PX-478 beyond its phase I clinical trial (NCT00522652) [70], and reports of toxicities such as neutropenia in mice treated with PX-478 [69], numerous other HIF1α inhibitors are in various stages of clinical trials [71], suggesting promising avenues for therapeutic applications.

There are several downstream mechanisms by which PLOD2 is reported to promote a pro-invasive phenotype, such as collagen remodeling [17, 18], enhancing cell motility through integrin stabilization [20], and induction of EMT [19, 22]. RNA sequencing of PLOD2-knockdown cells did not indicate expression changes in genes relating to these processes, however it did reveal a highly significant association between PLOD2 and the long non-coding RNA (lncRNA) LNCSRLR. Although unable to encode their own proteins, a plethora of lncRNAs have been identified as modulators of gene expression and cell signaling pathways, which in many instances can contribute to cancer progression under pathophysiological conditions [72]. In our study, we reveal that the expression of LNCSRLR is promoted downstream of PLOD2, and that their expression is strongly associated with each other clinically. To our knowledge, this is first time LNCSRLR expression has been linked to PLOD2.

Little is known regarding the function and regulation of LNCSRLR, having only been recently characterized as a mediator of sorafenib resistance in renal cell carcinoma [46]. Our functional investigation identifying LNCSRLR as a pro-invasive RNA corroborates similar results of a study in hepatocellular carcinoma [35]; however, it remains unclear how LNCSRLR promotes invasion. As lncRNAs can modulate gene expression at the level of translation, future studies will be required to investigate its potential effects at the protein level. Likewise, LNCSRLR is likely only one of several factors contributing to the pro-invasive phenotype of PLOD2, and it is reasonable to assume that PLOD2 interacts with other proteins post-translationally to promote invasion [20].

In conclusion, our results reveal PLOD2 as a negative prognostic factor for biochemical relapse that promotes migration and invasion in a diversity of prostate cancer cell types. In vivo, we confirm that PLOD2 plays a direct role in facilitating cancer cell extravasation. Mechanistically, HIF1α is upregulated in our radiorecurrent prostate cancer cells and promotes the expression of PLOD2; LNCSRLR is expressed downstream of PLOD2 and contributes a pro-invasive phenotype, thereby establishing a novel HIF1α-PLOD2-LNCSRLR regulatory axis conferring metastatic propensity to our radiorecurrent prostate cancer cells. Finally, we demonstrate the clinical promise of HIF1α inhibitors in mitigating metastasis, by inhibiting this regulatory axis to reduce migration, invasion, and extravasation in radiorecurrent prostate cancer with HIF1α inhibitor PX-478. Together, our findings pave the way for future preclinical and clinical studies focused on reducing metastatic propensity by targeting PLOD2, to ultimately enhance survival outcomes for patients with radiorecurrent prostate cancer.

DATA AVAILABILITY

The differentially expressed genes from our RNA sequencing analysis are uploaded as a separate Microsoft Excel file in the supplementary information files. RNA sequencing data has been deposited to the Sequence Read Archive (SRA) at the National Center for Biotechnology Information (NCBI) under PRJNA1139134. Otherwise, all data generated or analyzed during the current study are included in this published article.

REFERENCES

1. Rebello RJ, Oing C, Knudsen KE, Loeb S, Johnson DC, Reiter RE, et al. Prostate cancer. Nat Rev Dis Primers. 2021;7:9.
2. Wong MC, Goggins WB, Wang HH, Fung FD, Leung C, Wong SY, et al. Global incidence and mortality for prostate cancer: analysis of temporal patterns and trends in 36 countries. Eur Urol. 2016;70:862–74.
3. Draisma G, Boer R, Otto SJ, van der Cruijsen IW, Damhuis RA, Schröder FH, et al. Lead times and overdetection due to prostate-specific antigen screening: estimates from the European Randomized Study of Screening for Prostate Cancer. J Natl Cancer Inst. 2003;95:868–78.

4. Philipson RG, Romero T, Wong JK, Stish BJ, Dess RT, Spratt DE, et al. Patterns of clinical progression in radiorecurrent high-risk prostate cancer. Eur Urol. 2021;80:142–6.
5. Posdzich P, Darr C, Hilser T, Wahl M, Herrmann K, Hadaschik B, et al. Metastatic prostate cancer-a review of current treatment options and promising new approaches. Cancers (Basel). 2023;15:461.
6. Elmehrath AO, Afifi AM, Al-Husseini MJ, Saad AM, Wilson N, Shohdy KS, et al. Causes of death among patients with metastatic prostate cancer in the US From 2000 to 2016. JAMA Netw Open. 2021;4:e2119568.
7. Siegel DA, O'Neil ME, Richards TB, Dowling NF, Weir HK. Prostate cancer incidence and survival, by stage and race/ethnicity - United States, 2001-2017. MMWR Morb Mortal Wkly Rep. 2020;69:1473–80.
8. Bray F, Ferlay J, Soerjomataram I, Siegel RL, Torre LA, Jemal A. Global cancer statistics 2018: GLOBOCAN estimates of incidence and mortality worldwide for 36 cancers in 185 countries. CA Cancer J Clin. 2018;68:394–424.
9. Hanahan D, Weinberg RA. Hallmarks of cancer: the next generation. Cell. 2011;144:646–74.
10. Fares J, Fares MY, Khachfe HH, Salhab HA, Fares Y. Molecular principles of metastasis: a hallmark of cancer revisited. Signal Transduct Target Ther. 2020;5:28.
11. Polyak K, Weinberg RA. Transitions between epithelial and mesenchymal states: acquisition of malignant and stem cell traits. Nat Rev Cancer. 2009;9:265–73.
12. Winkler J, Abisoye-Ogunniyan A, Metcalf KJ, Werb Z. Concepts of extracellular matrix remodelling in tumour progression and metastasis. Nat Commun. 2020;11:5120.
13. Vilalta M, Rafat M, Graves EE. Effects of radiation on metastasis and tumor cell migration. Cell Mol Life Sci. 2016;73:2999–3007.
14. Fotouhi Ghiam A, Taeb S, Huang X, Huang V, Ray J, Scarcello S, et al. Long non-coding RNA urothelial carcinoma associated 1 (UCA1) mediates radiation response in prostate cancer. Oncotarget. 2017;8:4668–89.
15. Kurganovs N, Wang H, Huang X, Ignatchenko V, Macklin A, Khan S, et al. A proteomic investigation of isogenic radiation resistant prostate cancer cell lines. Proteomics Clin Appl. 2021;15:e2100037.
16. Terajima M, Taga Y, Nakamura T, Guo HF, Kayashima Y, Maeda-Smithies N, et al. Lysyl hydroxylase 2 mediated collagen post-translational modifications and functional outcomes. Sci Rep. 2022;12:14256.
17. Eisinger-Mathason TS, Zhang M, Qiu Q, Skuli N, Nakazawa MS, Karakasheva T, et al. Hypoxia-dependent modification of collagen networks promotes sarcoma metastasis. Cancer Discov. 2013;3:1190–205.
18. Du H, Chen Y, Hou X, Huang Y, Wei X, Yu X, et al. PLOD2 regulated by transcription factor FOXA1 promotes metastasis in NSCLC. Cell Death Dis. 2017;8:e3143.
19. Xu F, Zhang J, Hu G, Liu L, Liang W. Hypoxia and TGF-β1 induced PLOD2 expression improve the migration and invasion of cervical cancer cells by promoting epithelial-to-mesenchymal transition (EMT) and focal adhesion formation. Cancer Cell Int. 2017;17:54.
20. Ueki Y, Saito K, Iioka H, Sakamoto I, Kanda Y, Sakaguchi M, et al. PLOD2 Is Essential to Functional Activation of Integrin β1 for Invasion/Metastasis in Head and Neck Squamous Cell Carcinomas. iScience. 2020;23:100850.
21. Liu T, Xiang W, Chen Z, Wang G, Cao R, Zhou F, et al. Hypoxia-induced PLOD2 promotes clear cell renal cell carcinoma progression via modulating EGFR-dependent AKT pathway activation. Cell Death Dis. 2023;14:774.
22. Tong Y, Qi Y, Xiong G, Li J, Scott TL, Chen J, et al. The PLOD2/succinate axis regulates the epithelial-mesenchymal plasticity and cancer cell stemness. Proc Natl Acad Sci USA. 2023;120:e2214942120.
23. Lan J, Zhang S, Zheng L, Long X, Chen J, Liu X, et al. PLOD2 promotes colorectal cancer progression by stabilizing USP15 to activate the AKT/mTOR signaling pathway. Cancer Sci. 2023;114:3190–202.
24. Du H, Pang M, Hou X, Yuan S, Sun L. PLOD2 in cancer research. Biomed Pharmacother. 2017;90:670–6.
25. Espiritu SMG, Liu LY, Rubanova Y, Bhandari V, Holgersen EM, Szyca LM, et al. The evolutionary landscape of localized prostate cancers drives clinical aggression. Cell. 2018;173:1003–13. e15
26. Sinha A, Huang V, Livingstone J, Wang J, Fox NS, Kurganovs N, et al. The proteogenomic landscape of curable prostate cancer. Cancer Cell. 2019;35:414–27. e6.
27. Chen S, Huang V, Xu X, Livingstone J, Soares F, Jeon J, et al. Widespread and functional RNA circularization in localized prostate cancer. Cell. 2019;176:831–43. e22
28. Bhandari V, Hoey C, Liu LY, Lalonde E, Ray J, Livingstone J, et al. Molecular landmarks of tumor hypoxia across cancer types. Nat Genet. 2019;51:308–18.
29. Lalonde E, Ishkanian AS, Sykes J, Fraser M, Ross-Adams H, Erho N, et al. Tumour genomic and microenvironmental heterogeneity for integrated prediction of 5-year biochemical recurrence of prostate cancer: a retrospective cohort study. Lancet Oncol. 2014;15:1521–32.
30. P'ng C, Green J, Chong LC, Waggott D, Prokopec SD, Shamsi M, et al. BPG: Seamless, automated and interactive visualization of scientific data. BMC Bioinformatics. 2019;20:42.
31. Chandran UR, Ma C, Dhir R, Bisceglia M, Lyons-Weiler M, Liang W, et al. Gene expression profiles of prostate cancer reveal involvement of multiple molecular pathways in the metastatic process. BMC Cancer. 2007;7:64.
32. You S, Knudsen BS, Erho N, Alshalalfa M, Takhar M, Al-Deen Ashab H, et al. Integrated classification of prostate cancer reveals a novel luminal subtype with poor outcome. Cancer Res. 2016;76:4948–58.
33. Network CGAR. The molecular taxonomy of primary prostate cancer. Cell. 2015;163:1011–25.
34. Drost J, Karthaus WR, Gao D, Driehuis E, Sawyers CL, Chen Y, et al. Organoid culture systems for prostate epithelial and cancer tissue. Nat Protoc. 2016;11:347–58.
35. Li G, Liu Y, Zhang Y, Xu Y, Zhang J, Wei X, et al. A novel ferroptosis-related long non-coding rna prognostic signature correlates with genomic heterogeneity, immunosuppressive phenotype, and drug sensitivity in hepatocellular carcinoma. Front Immunol. 2022;13:929089.
36. Kim Y, Williams KC, Gavin CT, Jardine E, Chambers AF, Leong HS. Quantification of cancer cell extravasation in vivo. Nat Protoc. 2016;11:937–48.
37. Noda T, Yamamoto H, Takemasa I, Yamada D, Uemura M, Wada H, et al. PLOD2 induced under hypoxia is a novel prognostic factor for hepatocellular carcinoma after curative resection. Liver Int. 2012;32:110–8.
38. Benton G, Arnaoutova I, George J, Kleinman HK, Koblinski J. Matrigel: from discovery and ECM mimicry to assays and models for cancer research. Adv Drug Deliv Rev. 2014;79-80:3–18.
39. Xu Y, Zhang L, Wei Y, Zhang X, Xu R, Han M, et al. Procollagen-lysine 2-oxoglutarate 5-dioxygenase 2 promotes hypoxia-induced glioma migration and invasion. Oncotarget. 2017;8:23401–13.
40. Koh MY, Spivak-Kroizman T, Venturini S, Welsh S, Williams RR, Kirkpatrick DL, et al. Molecular mechanisms for the activity of PX-478, an antitumor inhibitor of the hypoxia-inducible factor-1alpha. Mol Cancer Ther. 2008;7:90–100.
41. Palayoor ST, Mitchell JB, Cerna D, Degraff W, John-Aryankalayil M, Coleman CN. PX-478, an inhibitor of hypoxia-inducible factor-1alpha, enhances radiosensitivity of prostate carcinoma cells. Int J Cancer. 2008;123:2430–7.
42. Chen Y, Terajima M, Yang Y, Sun L, Ahn YH, Pankova D, et al. Lysyl hydroxylase 2 induces a collagen cross-link switch in tumor stroma. J Clin Invest. 2015;125:1147–62.
43. Chen Y, Guo H, Terajima M, Banerjee P, Liu X, Yu J, et al. Lysyl hydroxylase 2 is secreted by tumor cells and can modify collagen in the extracellular space. J Biol Chem. 2016;291:25799–808.
44. Wei X, Li S, He J, Du H, Liu Y, Yu W, et al. Tumor-secreted PAI-1 promotes breast cancer metastasis via the induction of adipocyte-derived collagen remodeling. Cell Commun Signal. 2019;17:58.
45. Jiang Y, Zhang H, Wang J, Liu Y, Luo T, Hua H. Targeting extracellular matrix stiffness and mechanotransducers to improve cancer therapy. J Hematol Oncol. 2022;15:34.
46. Xu Z, Yang F, Wei D, Liu B, Chen C, Bao Y, et al. Long noncoding RNA-SRLR elicits intrinsic sorafenib resistance via evoking IL-6/STAT3 axis in renal cell carcinoma. Oncogene. 2017;36:1965–77.
47. Wang Z, Fan G, Zhu H, Yu L, She D, Wei Y, et al. PLOD2 high expression associates with immune infiltration and facilitates cancer progression in osteosarcoma. Front Oncol. 2022;12:980390.
48. Stone KR, Mickey DD, Wunderli H, Mickey GH, Paulson DF. Isolation of a human prostate carcinoma cell line (DU 145). Int J Cancer. 1978;21:274–81.
49. Kaighn ME, Narayan KS, Ohnuki Y, Lechner JF, Jones LW. Establishment and characterization of a human prostatic carcinoma cell line (PC-3). Invest Urol. 1979;17:16–23.
50. Sramkoski RM, Pretlow TG, Giaconia JM, Pretlow TP, Schwartz S, Sy MS, et al. A new human prostate carcinoma cell line, 22Rv1. In Vitro Cell Dev Biol Anim. 1999;35:403–9.
51. Tai S, Sun Y, Squires JM, Zhang H, Oh WK, Liang CZ, et al. PC3 is a cell line characteristic of prostatic small cell carcinoma. Prostate. 2011;71:1668–79.
52. Gillet JP, Varma S, Gottesman MM. The clinical relevance of cancer cell lines. J Natl Cancer Inst. 2013;105:452–8.
53. Miserocchi G, Mercatali L, Liverani C, De Vita A, Spadazzi C, Pieri F, et al. Management and potentialities of primary cancer cultures in preclinical and translational studies. J Transl Med. 2017;15:229.
54. Di Russo S, Liberati FR, Riva A, Di Fonzo F, Macone A, Giardina G, et al. Beyond the barrier: the immune-inspired pathways of tumor extravasation. Cell Commun Signal. 2024;22:104.
55. Reymond N, d'Água BB, Ridley AJ. Crossing the endothelial barrier during metastasis. Nat Rev Cancer. 2013;13:858–70.

56. Gjaltema RAF, de Rond S, Rots MG, Bank RA. Procollagen lysyl hydroxylase 2 expression is regulated by an alternative downstream transforming growth factor β-1 activation mechanism. J Biol Chem. 2015;290:28465–76.
57. Rosell-García T, Palomo-Álvarez O, Rodríguez-Pascual F. A hierarchical network of hypoxia-inducible factor and SMAD proteins governs procollagen lysyl hydroxylase 2 induction by hypoxia and transforming growth factor β1. J Biol Chem. 2019;294:14308–18.
58. Luo Z, Tian M, Yang G, Tan Q, Chen Y, Li G, et al. Hypoxia signaling in human health and diseases: implications and prospects for therapeutics. Signal Transduct Target Ther. 2022;7:218.
59. Gray LH, Conger AD, Ebert M, Hornsey S, Scott OC. The concentration of oxygen dissolved in tissues at the time of irradiation as a factor in radiotherapy. Br J Radiol. 1953;26:638–48.
60. Horsman MR, Mortensen LS, Petersen JB, Busk M, Overgaard J. Imaging hypoxia to improve radiotherapy outcome. Nat Rev Clin Oncol. 2012;9:674–87.
61. Sørensen BS, Horsman MR. Tumor hypoxia: impact on radiation therapy and molecular pathways. Front Oncol. 2020;10:562.
62. Wicks EE, Semenza GL. Hypoxia-inducible factors: cancer progression and clinical translation. J Clin Invest. 2022;132:e159839.
63. Iommarini L, Porcelli AM, Gasparre G, Kurelac I. Non-canonical mechanisms regulating hypoxia-inducible factor 1 alpha in cancer. Front Oncol. 2017;7:286.
64. Moeller BJ, Cao Y, Li CY, Dewhirst MW. Radiation activates HIF-1 to regulate vascular radiosensitivity in tumors: role of reoxygenation, free radicals, and stress granules. Cancer Cell. 2004;5:429–41.
65. Lee J, Guo HF, Wang S, Maghsoud Y, Vázquez-Montelongo EA, Jing Z, et al. Unleashing the potential of 1,3-diketone analogues as selective LH2 inhibitors. ACS Med Chem Lett. 2023;14:1396–403.
66. Zuurmond AM, van der Slot-Verhoeven AJ, van Dura EA, De Groot J, Bank RA. Minoxidil exerts different inhibitory effects on gene expression of lysyl hydroxylase 1, 2, and 3: implications for collagen cross-linking and treatment of fibrosis. Matrix Biol. 2005;24:261–70.
67. Wigerup C, Påhlman S, Bexell D. Therapeutic targeting of hypoxia and hypoxia-inducible factors in cancer. Pharmacol Ther. 2016;164:152–69.
68. Zhu Y, Zang Y, Zhao F, Li Z, Zhang J, Fang L, et al. Inhibition of HIF-1α by PX-478 suppresses tumor growth of esophageal squamous cell cancer in vitro and in vivo. Am J Cancer Res. 2017;7:1198–212.
69. Welsh S, Williams R, Kirkpatrick L, Paine-Murrieta G, Powis G. Antitumor activity and pharmacodynamic properties of PX-478, an inhibitor of hypoxia-inducible factor-1alpha. Mol Cancer Ther. 2004;3:233–44.
70. Tibes R, Falchook G, Von Hoff D, Weiss G, Iyengar T, Kurzrock R, et al. Results from a phase I, dose-escalation study of PX-478, an orally available inhibitor of HIF-1α. J Clin Oncol. 2010;28:3076.
71. Fallah J, Rini BI. HIF inhibitors: status of current clinical development. Curr Oncol Rep. 2019;21:6.
72. Statello L, Guo CJ, Chen LL, Huarte M. Gene regulation by long non-coding RNAs and its biological functions. Nat Rev Mol Cell Biol. 2021;22:96–118.
73. Frame G, Leong H, Haas R, Huang X, Wright J, Boutros PC, et al. Investigating PLOD2 as a therapeutic target to overcome metastasis in radiorecurrent prostate cancer. Cancer Res. 2024;84:1274.

ACKNOWLEDGEMENTS

We would like to thank Dr. Dennis Lee and the laboratory of Dr. Sascha Drewlo for kindly providing access to their hypoxic incubator. We would also like to thank the American Association for Cancer Research (AACR) and the Metastasis Minisymposium Chairs for the opportunity to present an overview of this research as an oral presentation at the 2024 AACR Annual Meeting [73].

AUTHOR CONTRIBUTIONS

GF, HL, RH, MD, UE, PCB, TK, SKL contributed to study design. GF, HL, RH, XH, JW, performed the experiments. GF, RH performed data analysis and figure preparation. GF wrote the initial draft of the manuscript. HL, MD, UE, PCB, TK, SKL supervised the research. All authors edited and approved the final version of the manuscript.

FUNDING

SKL acknowledges the very kind support provided by Wayne and Maureen Squibb. GF is supported by the Canada Graduate Scholarship-Master's (CGS-M) from the Canadian Institute of Health Research, The Strategic Training in Transdisciplinary Radiation Science for the 21st Century Program (STARS21) co-funded by Princess Margaret Research (PMR) and the Radiation Medicine Program (RMP) at UHN, and by the Queen Elizabeth II Graduate Scholarship in Science and Technology (QEII-GSST) funded by the Terry Fox Program, Sunnybrook, the Province of Ontario and the University of Toronto. SKL and TK received research funding from Prostate Cancer Canada Movember Discovery Grant (D2017- 1811), and Project Grants from the Canadian Institute of Health Research (PJT-162384; PJT-189979). This research is also funded by the Canadian Cancer Society Challenge Grant (grant #708133). SKL received research funding from Prostate Cancer Canada Movember Rising Star (RS2014-03), and the Prostate Cancer Fight Foundation/Ride for Dad. RH is supported by EMBO Postdoctoral Fellowship ALTF (1131-2021) and the Prostate Cancer Foundation Young Investigator Award (22YOUN32). PCB is supported by Prostate Cancer Foundation (20CHAS0), Early Detection Research Network (1U2CCA271894-01 and 3U01CA214194-0552) and NIH Informatics Technology for Cancer Research (ITCR) (1U24CA248265-01).

COMPETING INTERESTS

PCB sits on the scientific advisory board of Intersect Diagnostics Inc., BioSymetrics Inc., Sage Bionetworks. All other authors declare no conflicts of interest.

ETHICS APPROVAL

Ethics approval and written informed consent was obtained for the use of patient samples in accordance with the Declaration of Helsinki. Patient biopsy and cell derivation was performed under a Sunnybrook Health Sciences Centre approved Research Ethics Board study (REB#3463). All experimental protocols were performed in accordance with the institutional guidelines of Sunnybrook Health Sciences Centre.

ADDITIONAL INFORMATION

Supplementary information The online version contains supplementary material available at https://doi.org/10.1038/s44276-024-00085-3.

Correspondence and requests for materials should be addressed to Stanley K. Liu.

Reprints and permission information is available at http://www.nature.com/reprints

Publisher's note Springer Nature remains neutral with regard to jurisdictional claims in published maps and institutional affiliations.